Journal of Materials Chemistry A

Accepted Manuscript

ROYAL SOCIETY OF CHEMISTRY

www.rsc.org/materialsA

Journal of Materials Chemistry A RSCPublishing

PAPER

Atomic Layer Deposition of epitaxial CeO_2 thin layers for faster surface hydrogen oxidation and faster bulk ceria reduction / oxidation.

Cite this: DOI: 10.1039/x0xx00000x

Received 00th January 2015,
Accepted 00th January 2015

DOI: 10.1039/x0xx00000x

www.rsc.org/

Adrien Marizy,[a] Pascal Roussel,[b] Armelle Ringuedé[a] and Michel Cassir[a]

Thin ceria layers of 120 nm were processed by atomic layer deposition on both YSZ(100) single crystal substrates and polycrystalline YSZ ones. The CeO_2 layer deposited on the oriented substrate proved to be epitaxial after a low temperature annealing used to remove some crystallisation defects. The quality of the film was characterized by scanning electron microscopy and High Resolution X-ray diffraction. An electrochemical characterization under nitrogen and hydrogen atmosphere was carried out by electrochemical impedance spectroscopy (EIS). EIS measurements clearly show enhanced ceria reduction when the layer was epitaxial compared with the non-oriented CeO_2 layer. Moreover, the reoxidation process of the CeO_2 layer appears to be faster for the fully oriented sample. All those results are very promising to process orientation-controlled ceria surfaces for the catalysis of hydrogen oxidation inside SOFC devices but also for specific applications which need on a high rate of ceria reduction/reoxidation over several cycles.

Introduction

The unique benefits of Atomic Layer Deposition (hereafter ALD) to process SOFC layers have already been mentioned in the literature concerning ultrathin layers or interlayers acting as diffusion barriers, protective films or catalysts in micro-SOFC layers[1]. A ceria or doped-ceria interlayer between the electrolyte and the electrodes prevents the phases from mixing and constitutes a good cation diffusion barrier. At the cathode, ceria interlayer enhances the oxygen incorporation into the electrolyte[2] and at the anode, as an oxygen supplier, it is a good catalyst for hydrogen oxidation. Ceria is also potentially interesting for direct methane oxidation as it can prevent carbon deposition[3–6]. When deposited as a thin layer, polycrystalline ceria mainly exposes its most stable (111) orientation on the surface of the deposit. This (111) orientation proves to be poorly reactive as an oxidizer. It has been shown by DFT modelling and experiments carried out by Temperature Programed Reduction (TPR) that the orientation of ceria particles has a significant effect on their surface catalytic properties[4]. It is therefore important to control the surface orientation of ceria thin layers in order to reduce the SOFC working temperature and improve the fuel consumption efficiency. As already shown by Coll et al.[7] and by our team[8], (100) epitaxial CeO_2 thin films measuring up to 30 nm can be deposited onto YSZ(100). In this work, thicker (100) epitaxial layers of CeO_2 measuring 120 nm were processed by ALD at a higher growth speed than what has been reported previously. These layers, deposited onto single crystal and polycrystalline YSZ, were characterized by impedance spectroscopy and show a promising enhancement of the reduction of ceria thanks to (100) oriented ceria thin layers. Moreover, oriented layers re-oxidize faster than non-oriented CeO_2 layers while still maintaining their quality and orientation even after 10 days of measurements.

Experimental

Fabrication of the film

Ceria films were deposited in a Picosun Sunale R200 vertical flow type reactor using commercial $Ce(thd)_4$ (STREM chemicals) as cerium precursor. Ozone (70%) was used as an oxidizing source and was produced by a USA generator out of high purity oxygen. High purity N_2 was used as a carrier and purge gas. The temperature of the reaction chamber was set to 300°C and the precursor was warmed up to 180°C. The pulsing

[a]PSL Research University, Chimie ParisTech - CNRS, Institut de Recherche de Chimie Paris, 75005 Paris, France. E-mail: michel.cassir@chimie-paristech.fr

[b]Unité de Catalyse et Chimie du Solide - UMR CNRS 8181 Ecole Nationale Supérieure de Chimie de Lille Bat C7a - BP 90108, F-59652 Villeneuve d'Ascq, France

sequence is $Ce(thd)_4$ / N_2 / O_3 / N_2 with 3 / 5 / 4.5 / 5 s as pulsing times according to our previous work[8] but, for the present study, the nitrogen flow was boosted at 700 sccm during the pulsing time of $Ce(thd)_4$. One-side polished monocrystalline 10x10x0.5 mm^3 YSZ (100) doped at 9.5 mol% from Crystal Gmbh and home-made round-shaped polycrystalline YSZ (about 10x0.5mm, doping 8% - from commercial Tosoh powder) were used as substrates. One side of the substrates was covered with a Pt ink before the deposit to avoid any structural modification of the deposited layer during the annealing of the Pt ink. The ceria deposit was processed at 300°C.

Evaluation of the structural and microstructural quality of the thin film

The structural characterization of the deposited ceria thin films was carried out on a Rigaku Smartlab rotated anode X-Ray diffractometre for epitaxial samples and on a Panalytical Xpert (sealed tube) diffractometre for polycrystalline sample, both using Cu $K\alpha_1$ (1.5406 Å) wavelength. The thickness of the deposits was found to be 120 nm ±5 nm by X-ray reflectivity and confirmed by a Su-70 Hitachi SEM-FEG.

Electrochemical characterization

Impedance spectroscopy measurements were carried out under nitrogen atmosphere and under a mixed nitrogen-hydrogen atmosphere. Concentration of hydrogen inside the nitrogen flow was set to 10%. A potentiostat AutoLab® PGSTAT-302N with a FRA module was used to perform the impedance data collection. The configuration used was a specific two-electrode configuration such as the one previously used in several of our works[9]: a gold mesh was used along with the Pt-coated side of the sample and a Pt point-type electrode in mechanical contact with the side of the ceria deposit. A 200 mV AC signal was applied without any offset of polarization. Impedance measurements were carried out in the 1 MHz – 10 Hz (or 1 Hz) frequency range. One substrate of CeO_2-deposited monocrystalline YSZ(100) and one substrate of CeO_2-deposited polycrystalline YSZ have undergone the same impedance procedure, namely, a warm up until 430°C under nitrogen, then a stabilization time of 10 hours, followed by a reduction with the insertion of H_2 at 430°C and finally a reoxidation at 500°C under nitrogen. A program was set up to take measurements periodically in order to follow the temporal evolution of the reduction and of the re-oxidation.

Results and Discussion

Structure of the layers

A SEM-FEG observation of the samples in figure 1 reveals a highly conformal CeO_2 layer covering the grains of the polycrystalline YSZ sample and the low-roughness surface of the YSZ(100). The cross section of the polycrystalline sample reveals a columnar structure with tightly-confined columns of cerium dioxide, as could be expected with the ALD technique.

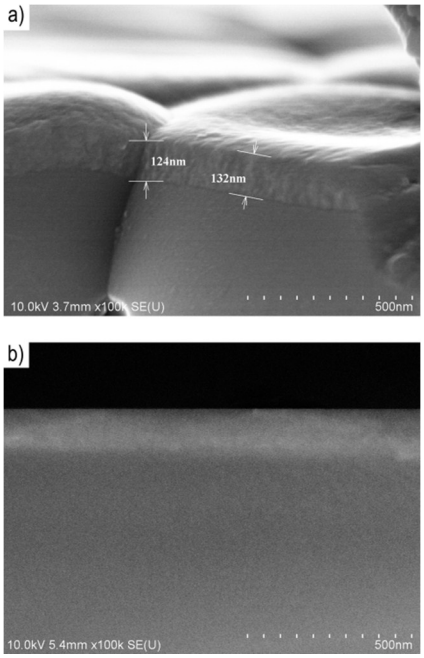

Fig. 1 SEM cross-section of CeO_2 deposited onto (a) polycrystalline YSZ and (b) a single YSZ(100) crystal. Note: thickness measurements on (a) are approximate due to the perspective artefact.

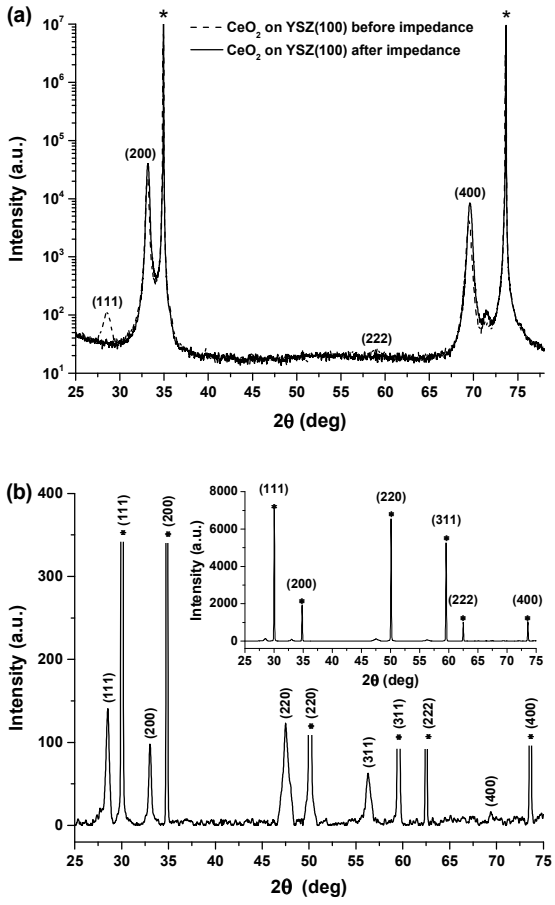

Fig. 2 XRD patterns of the 120 nm thick CeO_2 films grown on YSZ(100) (a) and on polycrystalline YSZ (b). The stars indicate the peaks of the substrates. In (b), the full XRD scan with labelled YSZ peaks is presented inside the inset. The main graph is a focus on the CeO_2 peaks.

The contrast between the CeO_2 layer and the YSZ (100) substrate is weak and suggests a good structural and chemical match between the substrate and the deposited layer. The size of the grains could be estimated to be 15 nm. Previous works reported a growth speed of 0.2 Å/cycle[7] and 0.06 Å/cycle[8]. Here, the growth rate is estimated at 0.36 Å/cycle for similarly dense and conformal films. This 6-fold increase in the growth rate is due to the 7-fold increase in the nitrogen flow during $Ce(thd)_4$ pulse, which changes the pressure inside the precursor bottle and allows more precursors per pulse to be sublimated and introduced inside the reactor chamber. This results in a better coverage of the surface of the sample at each pulse and thus an enhanced growth rate. The XRD patterns of the oriented and non-oriented layers, before and after impedance measurements are presented in figure 2. As can be seen, the XRD scan of the CeO_2 layer deposited on the polycrystalline substrate shows all the CeO_2 diffraction peaks, as expected, whereas the scan of the layer deposited onto the single YSZ(100) crystal shows only a few CeO_2 diffraction peaks: (200), (400), (111) and (222) before impedance but only (200) and (400) peaks after impedance. This very small (111) contribution did not appear in the previous works done with epitaxial CeO_2 onto YSZ(100)[7,8], but, either the thickness of the deposited thin films was a few nanometres or, for our previous layer of 30 nm, the growth speed was much lower (0.06 Å/cycle). This small (111) orientation was also present inside a 50 nm thick layer deposited also at 0.36 Å/cycle.

Nevertheless, this (111) XRD peak is weak and XRD analyses such as rocking curves and phi-scan, showed in figure 3, demonstrate that the as-deposited CeO_2 grains exposing their (100) plans are epitaxial toward the YSZ(100) substrates. Besides, this (111) peak is probably due to defects present inside the layer due to its significant thickness. Indeed, figure 3a, which is a comparison between these 120-nm-thick layers and thinner layers obtained in our previous work[8], shows that the rocking curve for the as-deposited layers is composed of two characteristic parts: a sharp one and a broader one. The sharp peak tends to disappear when the layer thickness increases. It can be inferred that the as-deposited layer is constrained by the lattice of the substrate near the YSZ(100) surface, as shown by this thin central part of the rocking curve. Nevertheless, the high lattice misfit (4.8% for cube-on-cube epitaxy of CeO_2 on YSZ) entails highly strained layers and, as the film grows, the influence of the substrate decreases (seen in the broader part of the rocking curve) and misfit dislocations may occur to relieve the strain. These defects are probably responsible for the small (111) XRD peak. After the impedance analyses, this thin part of the rocking curve is no longer present indicating a probably fully-relaxed layer toward the substrate. Moreover, the FWHM has decreased (1.6° before impedance and 1.1° after) indicating a better orientation of the grains. This probably occurs during the first 10 hours when the temperature rose to 430°C, which is above the deposition temperature (300°C), and therefore annealed the film, eliminating the defects and, thus, the (111) orientation observed by XRD. This fairly good common orientation of the ceria grains is confirmed by the phi-scan where the reflections of the layer are very well aligned with those of the substrate, thus indicating that the relaxed layer shows a cube-on-cube epitaxy without any rotation of the CeO_2 lattice in comparison with the substrate one.

In this work, the achievement lies in the fabrication of more than one hundred nanometres thick, epitaxial and highly conformal layers with a good growth speed considering the ALD technique used. Moreover, the as-deposited layer is nearly epitaxial and only a simple post-deposit low-temperature annealing of a few hours is needed to remove small defects. This performance allows one to control the surface orientation of a large area of CeO_2 layers and not only of small nanoparticles, as previously done[4]. This leads one to consider practical surface catalytic applications inside SOFC for faster hydrogen oxidation at the anode side, as shown by the studies on nanoparticles. As hoped by Desaunay et al.[4], if we consider an IT-SOFC system, the working temperature (500-600°C) anneals the layer and preserves the orientation of the deposited ceria grains and even contributes to improving it. Other applications such as three-way automotive catalytic converters require the ability of ceria to quickly uptake or intake oxygen[10]. In those applications, the bulk ceria layer could be reduced

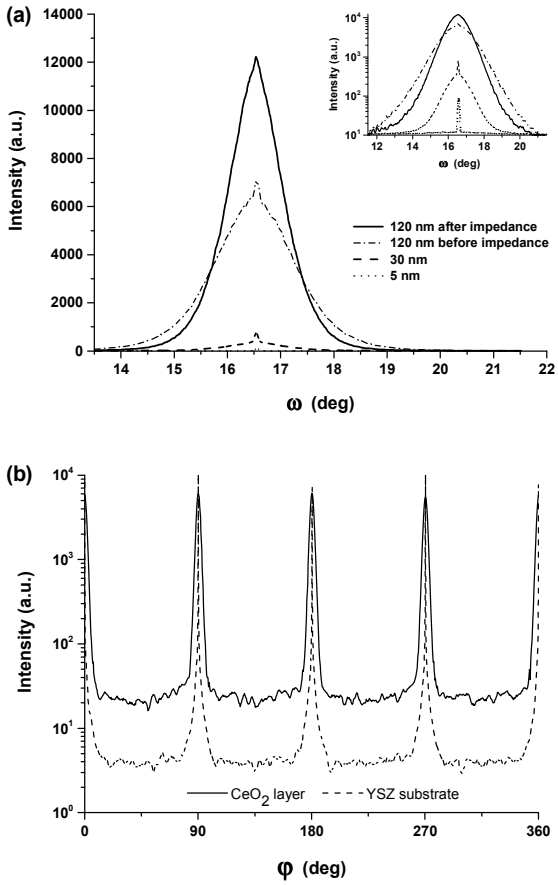

Fig. 3 (a) Rocking curves (ω scan) on the (200) plans (the same plot is presented in logarithmic scale inside the inset) and (b) ϕ scan at 2θ=47.48° corresponding to the (220) planes of the CeO_2 film (solid line) compared to ϕ scan at 2θ=50.08° corresponding to the (220) planes of the YSZ substrate (dashed line). The same diagram was obtained before and after impedance spectroscopy measurements.

without being constantly reoxidised by oxygen anions unlike inside a SOFC device. It is therefore relevant not only to study the surface catalytic reactivity but also to study the bulk reduction and oxidation of this oriented ceria layer compared with that of a non-oriented layer. EIS allowed us to study the bulk reactivity with hydrogen of this (100) oriented CeO_2 layer compared with the bulk reactivity of a non-oriented CeO_2 layer deposited on bulk polycrystalline YSZ.

Electrochemical characterization by impedance spectroscopy

Figure 4 presents the impedance diagrams for both oriented and non-oriented samples, in a mixture of 10% of hydrogen diluted in nitrogen flow as a function of exposure time to the gas. Each acquisition takes about two minutes and the program includes a five-minute pause between the end of a measurement and the beginning of the next one. The first measurement presented in figure 4 is the initial response of the samples under nitrogen atmosphere and the response seems to be composed of two semi-circles, not easy to distinguish because of overlapping on the Nyquist diagram for CeO_2 deposited on YSZ(100). This is not the case for CeO_2 on polycrystalline YSZ where only one badly defined semi-circle seems to be present within the same frequency range (~kHz to 1 MHz). The low frequency part (below 1 kHz), of the impedance diagrams is related to electrode reaction mechanisms, whatever the sample considered. This transition was checked by modifying the signal amplitude applied. Hydrogen is introduced within the nitrogen flow 10 s before the second measurement.

As can be seen in figure 4, for epitaxial CeO_2, the second semi-circle between roughly 1 kHz and 100 kHz is collapsing during the measurement period leading to an elongated loop formed with the electrode reaction. This leads to conclude that the second semi-circle is characteristic of the CeO_2 layer and the first smaller one is characteristic of the substrate even if both contributions are mixed. The third measurement (the second under hydrogen) shows only one semi-circle with a resistance decreasing only slightly over the following measurements but staying around 90 kΩ. CeO_2 was reduced by hydrogen during the second measurement and the remaining perfect semi-circle is the response of the monocrystalline YSZ(100) substrate. As can be seen from the phase Bode diagram, when the layer is reduced, the phase is very stable at 0° between 10 Hz and 10 kHz and the whole Bode diagram is characteristic of a first-order system representing the single crystal. Once the evolution is complete, the activation energy is indeed the same as that of the substrate (measured at 1.1 eV for monocrystalline YSZ(100)). At this temperature ceria is known to be reduced by hydrogen until it reaches a stabilised state at $CeO_{1.8}$[11]. In our case, the ceria layer is expected to be reduced when there is no more evolution between each impedance measurement. The layer becomes an electronic conductor and acts as an electrode, while the Pt point acts mainly as a current collector. In the case

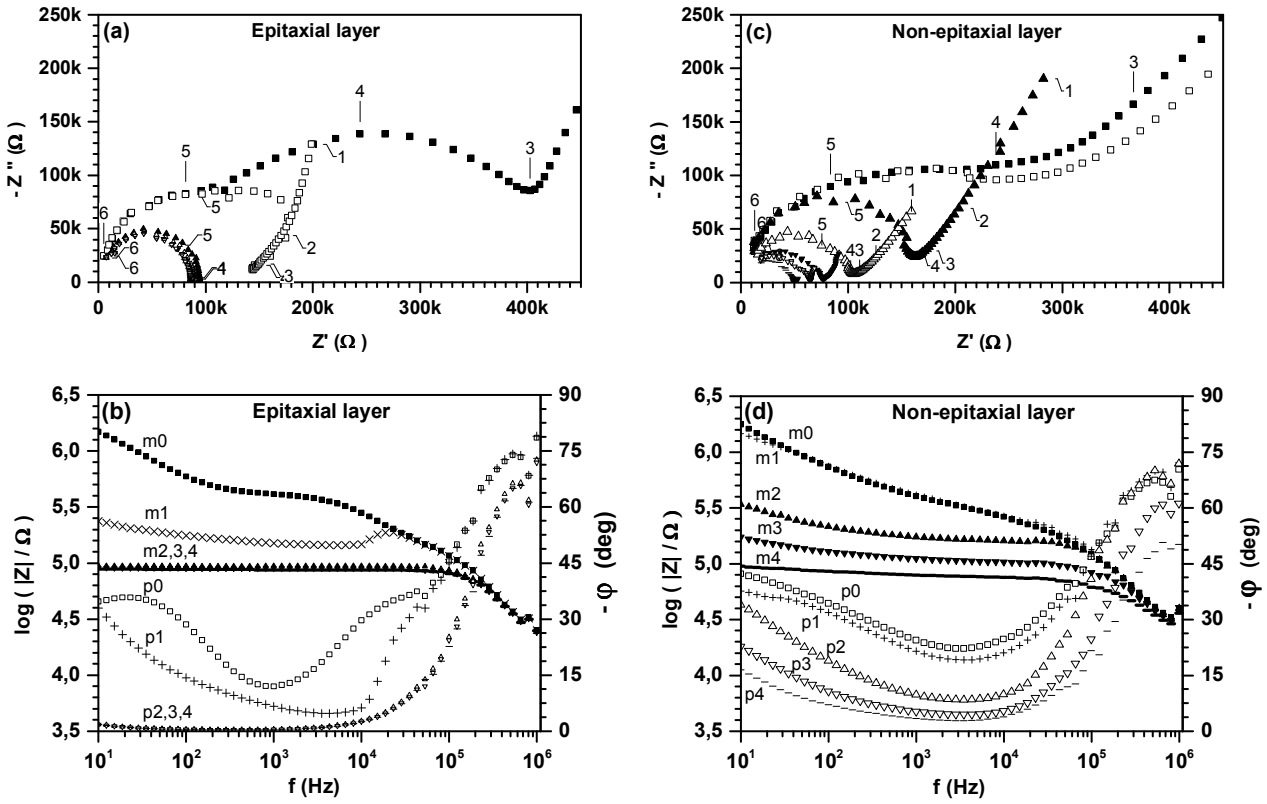

Fig. 4 Nyquist and Bode diagrams of (a) and (b) CeO_2 onto YSZ(100) and (c) and (d) onto polycrystalline YSZ during the reduction process of the CeO_2 layer at 430°C under a mixed hydrogen/nitrogen atmosphere (10% of hydrogen). Each measurement is separated by 7 minutes and hydrogen is introduced 10 s before the second measurement. For Bode diagrams, the Z module is indicated with a m index and the phase with a p index; index 0 indicates the first measurement. For Nyquist diagrams, the logarithm of the frequencies is indicated with numbers (6=10^6 Hz for example); full and empty markers alternate, starting with full square markers.

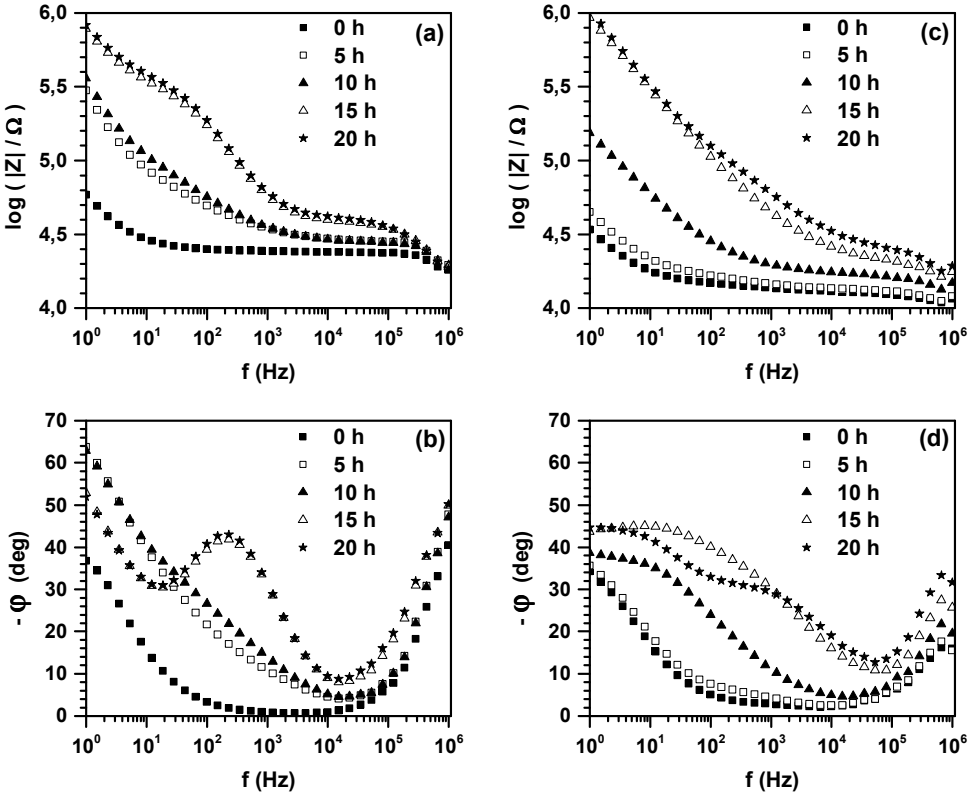

Fig. 5 Bode diagrams of (a) CeO_2 onto YSZ(100) and (b) onto polycrystalline YSZ during the re-oxidation process of the CeO_2 layer at 500°C under nitrogen atmosphere. Each measurement presented is separated by 5 hours.

of the reduction by hydrogen of the CeO_2 layer onto polycrystalline YSZ, the huge single semi-circle resistance tends to stabilize at 70 kΩ after the fourth measurement under hydrogen (28 minutes). The significant point of this study is that the reduction process of the ceria layer can be observed on only one measurement period for the epitaxial layer but it takes up to 4 measurements under hydrogen to observe a near stable quasi complete semi-circle for the polycrystalline sample. This behaviour is even more visible when observing at the Bode diagrams; indeed, the module becomes stable with a variation inferior to 5% between each measurement from the third measurement under hydrogen for the epitaxial CeO_2 as only from the seventh measurement for the non-oriented CeO_2 layer. In terms of time, it means that the reduction of the layer takes roughly 42 minutes for the non-oriented CeO_2 layer but only 14 minutes for the epitaxial (100) oriented CeO_2 layer i.e. a factor of 3 between both kinetics of reduction taking the module decrease rate as indicative of the main reduction process. Regarding these results, CeO_2 reduction by hydrogen is much faster with oriented (100) epitaxial CeO_2 on YSZ(100) than with a polycrystalline non-oriented CeO_2 layer.

After the end of the reduction, the hydrogen flow was shut down and the samples were reoxidized at 500°C thanks to the small residual presence of O_2 inside the system. Measurements are taken every 5 hours and figure 5 shows the Bode diagrams of the evolution of this process. For the non-oriented CeO_2 layer, after few modifications during the first 5 hours, the main process of re-oxidation occurs during the next 15 hours. But, for the epitaxial ceria layer, a two-step process seems to appear from those measurements. Indeed, unlike for the non-oriented sample, quick modifications of the module and the phase occur during the first 5 hours and between 10 and 15 hours. These periods are separated with a period of 5 hours with very few changes in the Bode Diagram. This behaviour is quite surprising and requires further investigation, as no explanation has been found so far. Nevertheless, the re-oxidation process is almost complete when a new peak appears on the phase diagram (around 200 Hz for the epitaxial sample and 1 kHz for the non-oriented layer). This peak appears clearly fifteen hours after the beginning of the re-oxidation process for the oriented sample. On the contrary, this peak is less marked for the non-oriented layer and appears only after twenty hours of re-oxidation.

Hence, the re-oxidation process is also quicker for the epitaxial sample. It should be noticed that the measurements under nitrogen before reduction and after reoxidation are not equal but remain in the same order of magnitude. For example, the activation energy of this reoxidized epitaxial sample has 0.1 eV more than before reduction (1.45 eV instead of 1.35 eV before reduction), and the same goes for the polycrystalline sample (1.15 eV to 1.0 eV). This rise in the activation energy after reoxidation under nitrogen may be attributed to the formation of a lattice of CeO_2 with fewer oxygen vacancies, which are known for favouring the ionic conductivity of the CeO_2 layer.

Unfortunately, we could not measure the Ce^{3+} content of the reduced/reoxidized ceria layer but such comparison would be very instructive to understand the process involved in this higher ceria reduction/oxidation rate with the epitaxial sample.
The results on the bulk reduction / oxidation of ALD epitaxial ceria layers are very promising for the treatment of exhaust gases from combustion engines where ceria provides oxygen buffering capacity during the oscillation between oxygen-deficient phase with a lot of hydrocarbons or CO to oxidize and oxygen-excess phase during which ceria uptakes oxygen and regenerates[10].

Conclusion

Highly conformal and dense epitaxial CeO_2 layers of up to 120 nm can be processed by ALD on YSZ(100). This allows one to process large area (100) oriented ceria surfaces which are known to act as a better catalyst than (111) oriented surface for the hydrogen oxidation reaction. Moreover, the epitaxial layer proves to be far more reactive when reduced by hydrogen than a polycrystalline one. Besides, the epitaxial layer re-oxidizes faster than the polycrystalline one. Finally after 10 days under measurement conditions and two additional reduction/oxidation cycles, the thin epitaxial layer seems not to be altered as far as its quality and its epitaxy are concerned, which leads to think that the epitaxial (100) CeO_2 layers could be used either as a good surface catalyst for hydrogen oxidation in SOFC or as a good oxygen provider and storing material, for example in exhaust gases converters where the enhanced reduction and oxidation rate of the epitaxial ceria layer could prove very useful. The perspective of a control over the orientation of the different layers composing the SOFC device is a hot topic[12] in which ALD could play a significant role, due to its ability to process a conformal deposit on micro tubular geometries[13]. Progress has been made in the process of Ni–YSZ cermet micro-tubes with a surface made up of lamellae perpendicular to the tube surface[14]. Provided that the crystalline surface orientation of those lamellae could be controlled, one could imagine to process epitaxial ceria tubular layers with ALD.

Acknowledgements

D. Chery and A. Meléndez-Ceballos for their contribution to the optimization of the deposition of CeO_2 layers by ALD. Imaging was performed on a Su-70 Hitachi SEM-FEG, the instrument facilitated by the IMPC (Institut des Matériaux de Paris Centre FR2482) financially supported by the C'Nano projects of the Region Ile-de-France.

Notes and references

1 M. Cassir, A. Ringuedé and L. Niinistö, *J. Mater. Chem.*, 2010, **20**, 8987–8993.
2 Z. Fan, C.-C. Chao, F. Hossein-Babaei and F. B. Prinz, *J. Mater. Chem.*, 2011, **21**, 10903.
3 T. Desaunay, Approche théorique et expérimentale pour la conception de nouveaux catalyseurs à base de CeO_2 pour l'anode des piles à combustibles, PhD thesis, UPMC Paris 6, France, 2012.
4 T. Désaunay, G. Bonura, V. Chiodo, S. Freni, J. P. Couzinié, J. Bourgon, a. Ringuedé, F. Labat, C. Adamo and M. Cassir, *J. Catal.*, 2013, **297**, 193–201.
5 B. C. Steele and A. Heinzel, *Nature*, 2001, **414**, 345–52.
6 R. J. Gorte and J. M. Vohs, *J. Catal.*, 2003, **216**, 477–486.
7 M. Coll, J. Gazquez, A. Palau, M. Varela, X. Obradors and T. Puig, *Chem. Mater.*, 2012, **24**, 3732–3737.
8 A. Marizy, T. Désaunay, D. Chery, P. Roussel, A. Ringuedé and M. Cassir, *ECS Trans.*, 2013, **57**, 983–990.
9 C. Brahim, F. Chauveau, A. Ringuedé, M. Cassir, M. Putkonen and L. Niinistö, *J. Mater. Chem.*, 2009, **19**, 760.
10 A. Trovarelli, M. Boaro, E. Rocchini, C. de Leitenburg and G. Dolcetti, *J. Alloys Compd.*, 2001, **323-324**, 584–591.
11 A. Laachir, V. Perrichon, A. Badri, J. Lamotte, E. Catherine, J. C. Lavalley, J. El Fallah, L. Hilaire, F. Le Normand, E. Quéméré, G.-N. Sauvion and O. Touret, *J. Chem. Soc. Faraday Trans.*, 1991, **87**, 1601–1609.
12 J. Santiso and M. Burriel, *J. Solid State Electrochem.*, 2011, **15**, 985–1006.
13 E. Eustache, P. Tilmant, L. Morgenroth, P. Roussel, G. Patriarche, D. Troadec, N. Rolland, T. Brousse and C. Lethien, *Adv. Energy*, 2014, **4**, 1–11.
14 R. Campana, a. Larrea, J. I. Peña and V. M. Orera, *J. Eur. Ceram. Soc.*, 2009, **29**, 85–90.

Atomic Layer Deposition of epitaxial CeO_2 thin layers for faster surface hydrogen oxidation and faster bulk ceria reduction / oxidation

Adrien Marizy[†], Pascal Roussel[‡], Armelle Ringuedé[†] and Michel Cassir*[,†]

[†] PSL Research University, Chimie ParisTech - CNRS, Institut de Recherche de Chimie Paris, 75005 Paris, France

[‡] Unité de Catalyse et Chimie du Solide - UMR CNRS 8181 Ecole Nationale Supérieure de Chimie de Lille Bat C7a - BP 90108, F-59652 Villeneuve d'Ascq, France